

Cyclic porphyrin dimers as hosts for coordinating ligands

G VAIJAYANTHIMALA^a, V KRISHNAN^{a,b,*} and S K MANDAL^a

^aDepartment of Inorganic and Physical Chemistry Indian Institute of Science, Bangalore 560 012

^bPresent address: Chemical Biology Unit of the Jawaharlal Nehru Centre for Advanced Scientific Research, Indian Institute of Science Campus, Bangalore 560 012

e-mail: vkrish@jnscar.ac.in

Abstract. Bicovalently linked tetraphenylporphyrins bearing dioxypentane groups at the opposite (transoid, H₄A) and adjacent (cisoid, H₄B) aryl groups have been synthesised. Protonation of the free-base porphyrins leads to fully protonated species H₈A⁴⁺/H₈B⁴⁺ accompanied by expansion of cavity size of the bisporphyrins. The electrochemical redox studies of these porphyrins and their Zinc(II) derivatives revealed that the first ring oxidation proceeds through a two-electron process while the second ring oxidation occurs at two distinct one-electron steps indicating unsymmetrical charge distribution in the oxidized intermediate. The axial ligation properties of the Zinc(II) derivatives of H₄A/H₄B with DABCO and PMDA investigated by spectroscopic and single crystal X-ray diffraction studies showed predominant existence of 1 : 1 complex. The Zn₂A·DABCO complex assumes an interesting eclipsed structure wherein DABCO is located inside the cavity between the two porphyrin planes with Zn–N distances at 2.08 and 2.22 Å. The Zn atoms are pulled into the cavity due to coordination towards nitrogen atoms of DABCO and deviate from the mean porphyrin plane by 0.35 Å. The electrochemical redox potentials of the axially ligated metal derivatives are found to be sensitive function of the relative coordinating ability of the ligands and the conformation of the hosts.

Keywords. Crystal structure; cyclic porphyrin dimers; host–guest complexes; solution conformation.

1. Introduction

There has been an increasing interest in the study of covalently linked bisporphyrins in view of their utility as models for the Reaction Centre complex of the photosynthetic system, as catalysts for H₂O₂ decomposition,¹ mimicking certain enzyme functions² and to evolve basic understanding for excitation energy and electron transfer reactions.³ The two porphyrin units linked through a single covalent linkage manifest in a multitude of conformers⁴ while bisporphyrins bearing more than one covalent linkage restrict the number of conformers that can be probed by different spectroscopies. The nature of the individual porphyrin units, the positions of the covalent attachment, the nature and the length of the linking groups play an important role in governing the properties of these porphyrins. Majority of the bisporphyrin systems reported were of octaalkylporphyrin derivatives.⁵ However, the syntheses of such systems involve multiple steps and lead to very low yields of

the desired products. The synthetic procedure of these entities require the formation of amide⁶ or ester⁷ linkages in the bridging units from the reaction of an acid chloride monomer with another monomer containing amine or alcohol chains under high dilution conditions. These dimers have unsubstituted *meso* positions which are susceptible to oxidation and hence render them unstable towards oxidising agents.⁸ On the other hand, *meso*-tetraphenylporphyrins are remarkable molecular candidates due to their ease of synthesis. A few cofacial bisporphyrin systems of *meso*-tetraphenylporphyrin have been reported with tetra-covalent linkage through phenyl groups.⁹ The first tetracovalently bridged cofacial bisporphyrin through a para-phenyl positions was reported by Kagan *et al.*¹⁰ and through meta-phenyl positions by Karaman *et al.*¹¹ Closely interspaced R-((TPP)H₂)₂ are relatively unknown with the exception of a few bisporphyrins.^{9,12} The metal (II) derivatives of covalently linked porphyrin dimers have attracted a wide interest in the molecular recognition research. Host–guest complexation of cofacial bisporphyrins and cyclic tris and tetraporphyrins have been reported in the literature.¹³

*For correspondence

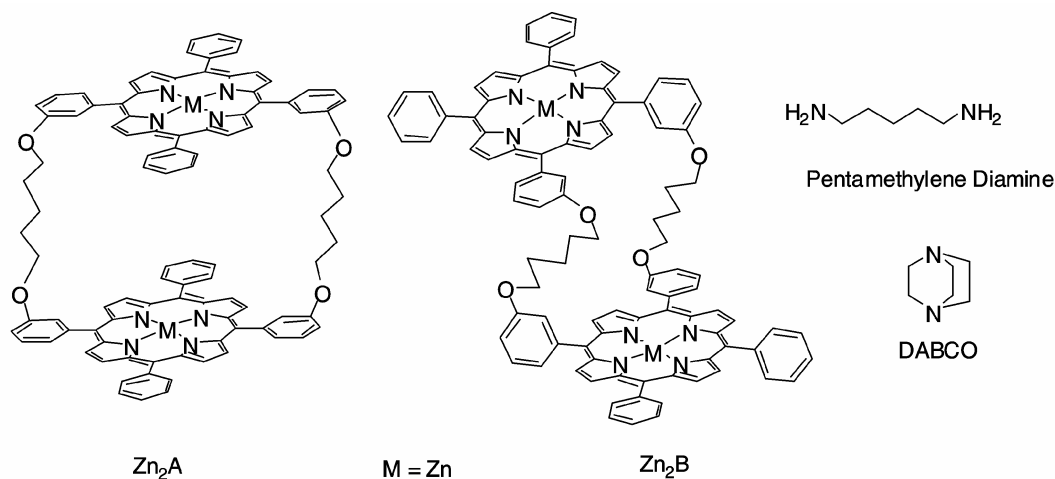


Figure 1. Structures of bicovalently linked bisporphyrins H_4A and H_4B . The axial ligands, 1,4-diazobicyclo[2,2,2]octane, DABCO and 1,5-pentamethylenediamine are shown.

2. Syntheses

We present here a method for the facile synthesis of two bisporphyrins in different molecular geometries by using the *meta-trans* and *meta-cis*-dihydroxyphenyl derivatives of meso-tetraphenylporphyrins. The porphyrins that were linked through *trans*-phenyl rings with pentanedioxy chains leads to bisporphyrin *trans*-(H_2TPP)₂, H_4A and the one linked through *cis*-phenyl groups yielded a *cis*-(H_2TPP)₂, H_4B (figure 1). The ability of zinc derivatives of these porphyrins to bind bidentate ligands, 1,4-diazobicyclo[2,2,2]octane (DABCO) and 1,5-pentamethylenediamine, (PMDA) inside the cavity is investigated and a structure of one of the complexes is reported here. The procedure adopted for the synthesis of bisporphyrins, H_4A and H_4B , linked with pentanedioxy ($n = 5$) chain at high dilution conditions ($\sim 10^{-5}$ M) resulted in fairly good yield ($\sim 12\%$) of the products. Attempts to synthesise bisporphyrins with short linkages ($n = 2, 3$ and 4) resulted in the formation of open products with very low yields.

3. Experimental

Pyrrole (Fluka, Switzerland) was distilled over KOH pellets under reduced pressure. Benzaldehyde and *meta/para*-hydroxybenzaldehyde purchased from Aldrich were used without further purification. Pentamethylene dibromide procured from Aldrich Chemicals (USA) was used as received. The bidentate nitrogenous bases, DABCO (1,4-diazobicyclo[2,2,2]octane) PMDA (1,5-pentamethylenediamine) procured

from Ranbaxy chemical company, India were of high purity are used as received.

The solvents were dried and distilled before use. The spectral and electrochemical redox measurements were carried out on instruments described elsewhere.²⁴ Proper precautions were taken not to expose the solutions to bright light. Prior to spectral measurements, the solutions were purged with argon.

3.1 Synthesis of bisporphyrins

The synthetic strategy employed here is to couple the 5,10/15,15-*bis*(3'-hydroxyphenyl)-15,20/10,20-diphenylporphyrins with the corresponding preformed dipentamethylenebromide derivatives under high dilution reaction conditions.

3.1a 5,10/5,15-*bis*(3'-hydroxyphenyl)-15,20/10,20-diphenylporphyrin: The *cis/trans*-dihydroxyphenyl-diphenylporphyrins are synthesised by refluxing benzaldehyde (2.08 g, 0.02 mmol), *meta*-hydroxybenzaldehyde (2.45 g, 0.02 mmol) and pyrrole (2.72 g, 0.04 mmol) in propionic acid (300 cm³) for 45 min. After the workup, the reaction mixture was subjected to TLC in 10 : 1 (v/v) CHCl₃: acetone mixture. The six spots with relative R_f values of 0.79, 0.69, 0.58, 0.50, 0.31 and 0.12 corresponding to TPP (1), 5-(3'-hydroxyphenyl)-10,15,20-triphenylporphyrin (2), 5,15-*bis*(3'-hydroxyphenyl)-10,20-diphenyl porphyrin (3), 5,10-*bis*(3'-hydroxyphenyl)-15,20-diphenylporphyrin (4), 5,10,15-*tris*(3'-hydroxyphenyl)-20-phenylporphyrin (5) and 5,10, 15,20-tetrakis(3'-hydroxyphenyl)porphyrin (6) respectively were found. The

separation of these porphyrins is accomplished by column chromatography employing a short column (5 × 60 cm) containing activated silica gel. By careful change of the composition of eluting solvent mixture, **3** (0.15 g, 2.4%), **4** (0.23 g, 3.7%) and **5** (0.45 g, 7.1%) were separated using 1%, 2% and 3% of acetone in chloroform as solvent, respectively. The compounds are spectroscopically pure. ¹H NMR (200 MHz in CDCl₃, δ in ppm): **3** δ 8.88 (2d, 8H, *J* = 4.88 Hz, H(3), 8.20 (*m*, 4H, *o*-unsub.phenyl H), 7.77 (*m*, 6H, 12, *m*-unsub.phenyl H), 7.75–7.55 (*m*, 8H, sub.phenyl H), –2.81 (*s*, 2H, imino H); **4** δ 8.86 (2d, 2s, 8H, *J* = 3.88 Hz, H_β, 8.20 (*m*, 8H, sub.phenyl H), –2.81 (*s*, 2H, imino H), 7.75 (*m*, 6H, 12, *m*-unsub.phenyl H), 7.72–7.25 (*m*, 8H, sub.phenyl H), –2.81 (*s*, 2H, imino H); **5** δ 8.91 (*m*, 8H, H_β), 8.22 (*m*, 2H, *o*-unsub.phenyl H), 7.76 (*m*, 3H, *p,m*-unsub.phenyl H), 7.74–7.30 (*m*, 12H, sub.phenyl H), –2.77 (*s*, 2H, imino H).

3.1b *5,10/5,15-bis(3'-(1-bromopentyloxy)phenyl)-15,20/10,20-diphenylporphyrin*: The functionalised free-base porphyrin, *m-cis/trans*-dihydroxy porphyrin (0.2 g, 0.3 mmol) was dissolved in 100 cm³ of dry distilled acetone containing 1 g of anhydrous K₂CO₃. To this 1 cm³ of 1,5-dibromopentane [Br-(CH₂)₅-Br] was added and the reaction mixture was refluxed for a period of 48 h. Subsequent to the removal of solvent and washing the residue with water, it was dissolved in a minimum amount of CHCl₃ and chromatographed on a neutral alumina column using CHCl₃ as the eluent. The title compound was eluted as a first band (0.26g, 90%). ¹H NMR (200 MHz, in CDCl₃, δ in ppm) *m-trans*-H₂TPP(O-(1)CH₂-(2)CH₂-(3)CH₂-(4)CH₂-(5)CH₂-Br)₂: 8.82–8.90 (2d, *J* = 4.85 Hz, 8H, H_β), 8.19–8.23 (*m*, 4H, *Q*-unsub.phenyl-H), 7.77 (*m*, 6H, *m*, 12-unsub.phenyl H), 7.66–7.28 (*m*, 8H, subs.phenyl-H), 4.15 (*t*, *J* = 6.20 Hz, 4H, –OCH₂–), 3.43 (*t*, *J* = 6.66 Hz, 4H, –CH₂Br–), 1.91 (*m*, 8H, (2,4)CH₂–), 1.67 (*m*, 4H, –(3)CH₂–), –2.79 (*s*, 2H, imino H); *m-cis*-H₂TPP(O-(1)CH-(2)CH₂-(3)CH₂-(4)CH₂-(5)CH₂-Br)₂: 8.82–8.90 (2d, *J* = 4.85 Hz, 8H, H_β), 8.19–8.23 (*m*, 4H, *o*-unsub.phenyl H), 7.77 (*m*, 6H, *m*, 12-unsub.phenyl H), 7.68–7.58, 7.33–7.28 (*m*, 8H, subs.phenyl-H), 4.14 (*t*, *J* = 6.16 Hz, 4H, –OCH₂–), 3.42 (*t*, *J* = 6.65 Hz, 4H, –CH₂Br), 1.91 (*m*, 8H, –(2,4)CH₂–), 1.67 (*m*, 4H, –(3)CH₂–), –2.79 (*s*, 2H, imino H).

3.1c *Bi-covalently linked free-base bisporphyrins*: In a typical bisporphyrin synthesis, *m-cis/trans*-

H₂(TPP)(O(CH₂)₅Br)₂ (0.12 g, 0.13 mmol) and *m-cis/trans*-H₂(TPP)(OH)₂ (0.08 g, 0.13 mmol) were dissolved in dry DMF (100 cm³). This solution was added slowly to a stirring solution of DMF (1 dm³) containing K₂CO₃ (1 g) over a period of 12 h. The reaction mixture was stirred for a further period of 48 h. The reaction mixture was filtered and the solvent, DMF was removed under reduced pressure to obtain the purple solid. After the work up, the unreacted porphyrin dibromide was removed as a first band from column chromatography (silica gel) and the second band was subjected to preparative TLC on a 0.05 × 20 × 20 cm silica gel plate using toluene as the eluent. TLC showed a single band when the starting material used was *m-trans*-dihydroxy-porphyrin and it was collected to give bisporphyrin, H₄A (0.018 g, 10%). Several bands were observed on TLC when the starting material employed was *m-cis*-dihydroxyporphyrin derivatives. Each band was collected separately and characterised by ¹H NMR. The first non-polar band was collected to give the bisporphyrin, H₄B (0.022 g, 12%). The yields were based on the amount of dihydroxyphenylporphyrins employed in the reaction. FAB MASS showed a molecular ion peak (*m/z*) at 1431.00 (M + 1)[±] for H₄A or H₄B. (calc. C₉₈H₇₆O₄N₈ (M[±]) = 1429.71). The *R_f* values for H₄A and H₄B are 0.29 and 0.23 (toluene : Pet.ether, 2 : 1, v/v), respectively.

The zinc(II) derivatives of the bisporphyrins were prepared using the appropriate metal acetate as the metal carrier by procedures described in literature. The metallation of the bisporphyrins was followed by optical spectroscopy to ensure that both the porphyrin units are metallated. The yields were 90% based on the amount of free-base bisporphyrins used.

3.2 Methods

The protonation of the bisporphyrins was followed by optical and ¹H NMR spectroscopic methods. Solution (0.5 cm³) in CDCl₃ with porphyrin of known concentration (10⁻² M) were titrated directly in an NMR tube by successive addition of TFA (0.01–10 M) using a microliter syringe. The total volume change over a complete protonation sequence was negligible. After each addition, the solution was mixed and spectra were measured over the range –5 to +10δ.

The equilibrium constants, *K* for the complexation of zinc(II) derivatives of bisporphyrins with bidentate ligands, DABCO and PMDA have been

determined using optical absorption method at 298 K. All measurements were made using 1,2-dichloroethane as the solvent. The concentration of the bisporphyrins were maintained at 1×10^{-5} M, while the concentration of the base was varied from 1×10^{-5} M to 1×10^{-1} M. The equilibrium constants, K were evaluated from the change in absorbance of the Q transitions of zinc(II) bisporphyrins on increasing addition of base. Hill plots²⁵ were constructed using standard least square fit programs to determine stoichiometry of the complex and to evaluate the binding constant, K . The ^1H NMR spectral titration was performed on increasing addition of base to a bisporphyrin (1 mM) solution in CDCl_3 .

3.2a X-ray crystallographic data: Single crystals of this host-guest complex, $\text{Zn}_2\text{A-DABCO} \cdot 8\text{C}_2\text{H}_4\text{Cl}_2 \cdot \text{H}_2\text{O}$ was obtained by the slow evaporation of a $\text{Zn}_2\text{A} : \text{DABCO}$ (1 : 1.20) dichloroethane solution at ambient temperature.

3.2b Crystal data: $\text{C}_{120}\text{H}_{118}\text{N}_{10}\text{Zn}_2\text{Cl}_{12}$, $M = 2478.32$, monoclinic, space group $P2_1/c$, $a = 14.103(8)$ Å, $b = 18.673(9)$ Å, $c = 23.815(8)$ Å, $\beta = 107.11(4)^\circ$ ($V = 5994(5)$ Å³ (by least-squares refinement of 25 reflections), $\lambda = 0.7107$ Å, $Z = 2$, $D_c = 1.37$ g cm⁻³, red diamond shaped crystals, crystal dimensions $0.42 \times 0.41 \times 0.35$ mm, $\mu(\text{MoK}_\alpha) = 8.24$ cm⁻¹.

3.2c Data collection and processing: A CAD4 diffractometer; graphite-monochromated MoK_α radiation; 2θ scan mode; range 4° – 40° ; 5493 unique reflections; $R_{\text{merge}} = (0.0914)$; 3782 observed reflections with $I > 3\sigma(I)$ [$w = 1.0/\sigma^2(F_o)$]; 40% crystal decay.

3.2d Structure analysis and refinement: The structure was solved by direct methods using SHELXS-86²⁶ and the remaining atoms were located from difference Fourier maps. All hydrogen atoms were either located or put at the calculated positions with an isotropic thermal parameter of 0.1 (Å²) and were not refined. Carbon atoms of the DABCO were found to be positionally disordered and six sites were refined with a site occupancy factor (sof) of 0.5. Chlorine atoms of one of the dichloroethane molecules also were found to be positionally disordered and the four sites were refined with a sof of 0.5. Full matrix leastsquares refinement using SHELX-76 program²⁷ converged $R = 0.0914$ and $R_w = 0.0965$ [$2\theta = 4$ – 40° , $I > 3\sigma(I)$] and $w = 1.0/\sigma^2(F_o)$.

Additional material available from the Cambridge Crystallographic Data Centre comprises thermal parameters and remaining bond lengths and bond angles.

4. Results and discussion

The products were identified by FAB Mass and ^1H NMR spectroscopic methods. The ^1H NMR spectra of bisporphyrins, H_4A and H_4B are highly characteristic and furnish information on the possible conformations in solution (figure 2). The proton resonances of H_4A and H_4B occur in a shielded region relative to the monomeric H_2TPP indicative of the presence of ring current effect induced by the proximal disposition of two porphyrin units.^{9,14} The imino protons of the free-base porphyrin, H_4A resonate as a singlet at -3.14 ppm shifted upfield relative to the resonances of inner imino protons of monomeric H_2TPP (~ 2.71 ppm) while a multiplet (~ 2.94 ppm) was observed for H_4B relative to that of monomeric porphyrin suggest co-facial arrangement of the porphyrin units. Interestingly, the multiplet resonance around -2.94 ppm observed for H_4B is resolved to two broad singlets (-3.00 and -3.11 ppm), on lowering the temperature (-45°C) while under similar conditions, the singlet resonance observed for H_4A remain unaffected. The occurrence of two singlet resonances arises from chemical non-equivalence of the imino protons in H_4B due to the preferred location of the protons in each of the porphyrins unit. It may be pointed out here that in H_4B , the covalent linkages at the adjacent aryl groups make two of the pyrrole rings in each of the porphyrin unit distinct from the others.¹⁵ The single resonance observed for H_4A indicates that both the imino protons are equivalent. The pyrrolic protons of H_4A resonate as two distinct doublets at 8.69 and 8.62 ppm while a multiplet resonance around 8.81 ppm was observed for H_4B . The appearance of two doublets in H_4B is similar to those observed for *trans*-diaminophenyldiphenylporphyrin reported by Sun *et al*¹⁶. The multiplet resonance seen in H_4B arise essentially from the different conformations of H_4B due to the presence of flexible covalent linkages at the adjacent aryl groups and due to the non-equivalence of β -pyrrole protons. Interestingly, lowering of temperature results in absence of the multiplet resonance and appearance of two doublets for β -pyrrole protons, signaling the preferred conformation of H_4B . It is noteworthy that under similar con-

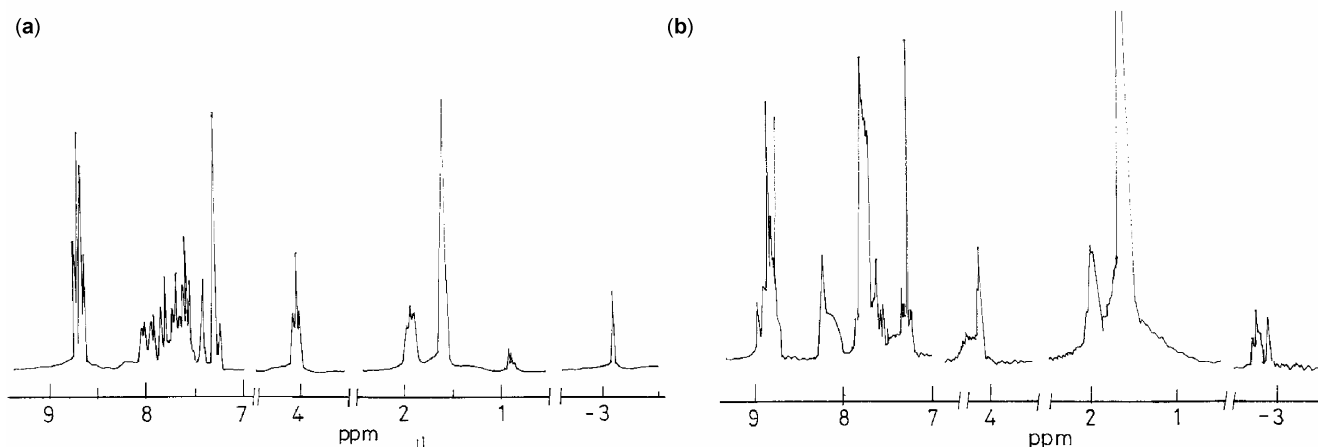


Figure 2. The ^1H NMR spectra of (a) H_4A and (b) H_4B in CDCl_3 at 298 K.

ditions, the pyrrole proton resonance of H_4A are not significantly affected, indicating that co-facial conformation persists at low temperature. The proton resonances of the *meso*-aryl groups of H_4A and H_4B are very instructive in arriving at the different orientational features. The four *ortho* protons ($2'$) in H_4A which are projecting inside the cavity resonate at 7.39 ppm while the other four *ortho* protons ($6'$) resonate as a multiplet at 7.80 ppm. The protons (2 and 6) of the unsubstituted aryl groups resonate as a multiplet centered around 8.02 ppm and 7.98 ppm respectively. The shielding effect experienced by the protons of the substituted *meso*-aryl groups ($2'$) indicates the influence of ring current arising from the face-to-face orientation of the porphyrin units.^{11,17} The resonance of phenyl protons of H_4B , however, appear as a complex multiplet and hence no detailed assignments are made. The assignment of the proton resonance of the bridging groups is largely aided by the spectra of the 2,5-dibromopentane (a) and the precursor complex, 5,10/5,15-bis[3'-(1-bromopentoxyphenyl)]-15,20/10,20-diphenylporphyrin (b). The bisporphyrins, H_4A and H_4B exhibit resonances of the bridging protons at 4.04 ppm (*t*) and at 1.90 ppm (*m*) corresponding to $-\text{OCH}_2^-$ and $(-\text{CH}_2-\text{CH}_2-\text{CH}_2-)$ protons. The observed proton resonance spectral results are indicative of the face to face conformation of porphyrin rings in H_4A and predominantly *endo-cis* orientation of the porphyrin rings in H_4B . The ^1H NMR spectra of the zinc(II) derivatives of H_4A and H_4B exhibit resonances similar to those of the multiplet structure of free-base indicating no major conformational change on metallation.

4.1 Protonation studies

Interesting results are obtained on protonation of these porphyrins. Typical spectra of acid titration of the bisporphyrins, H_4A and H_4B are shown in figures 3 and 4 respectively. It is found that addition of acid to the bisporphyrins results in the complete disappearance of the ring current induced shifts of proton resonances of β -pyrrole, imino and bridging methylene groups. The ^1H NMR spectra of H_4A and H_4B in less than four equivalents of acid (0.03 M) consists of resonances that can be ascribed to both free and fully protonated species, H_8P^{4+} (figures 3b and 4b). The absence of resonances at intermediate positions is ascribed to the absence of partially protonated intermediates, similar to that found for the H_2TPP and $(\text{DMA})_4\text{PH}_2$ [tetrakis(*p*-dimethylamino-phenyl)porphyrin]. The intensity ratio of resonances of H_8P^{4+} and H_4P increases with increase in concentration of the acid. The formation of fully protonated species is complete on addition of 4 equivalents of acid (0.05 M). The internal N–H proton resonance at 3.14 ppm in H_4A is shifted downfield to 0.18 ppm upon formation of H_8P^{4+} . As the concentration of TFA is increased beyond 0.05 M, the N–H resonance gradually moves towards upfield and in TFA solvent, this signal appears as a singlet at -2.25 ppm. The proton resonances that are followed are those of only inner imino nitrogens. Occasionally, it is difficult to locate the N–H protons on addition of acid (figure 2b). The position of the resonance has been resolved by deuteration experiments. Substantial changes are observed in the chemical shifts of $-\text{OCH}_2$, β -pyrrole and aromatic protons as the tetra-

protonation takes place. The resonance of β -pyrrole protons moves upfield from 8.64 ppm by 0.2 ppm and that of $-\text{OCH}_2$ protons shifted downfield by 0.3 ppm. These shifts in the proton resonances are in the directions to be expected if the aromatic ring current decreases on protonation. As the TFA concentration is increased beyond that necessary to form H_8P^{4+} , these signals again move continuously in opposite direction (figures 3c–f) with the resonances of H_β shifted downfield by 0.1 ppm and that of N–H protons shifted upfield by 2.10 ppm. The *meso*-aryl proton resonances are broadened signifi-

cantly, eventually with the disappearance of multiplet structure in TFA solution. The direction of proton resonance shifts on protonation of H_4B follows the same patterns as that observed for H_4A , however, the magnitude of the shifts of the resonances is quite different. Upon formation of H_8B^{4+} , the imino proton resonance at -2.91 ppm in H_4B shifted downfield to 0.32 ppm at 4 equiv of acid (0.05 M) (figure 3c). On increasing the concentration of TFA, the signal moves gradually upfield (figures 3d–f), and appears as a complex multiplet around -1.60 ppm in TFA solvent (figure 3g). The complex multiplicity and downfield shift of the resonances of imino protons of H_8B^{4+} , relative to that of H_8A^{4+} reveals that

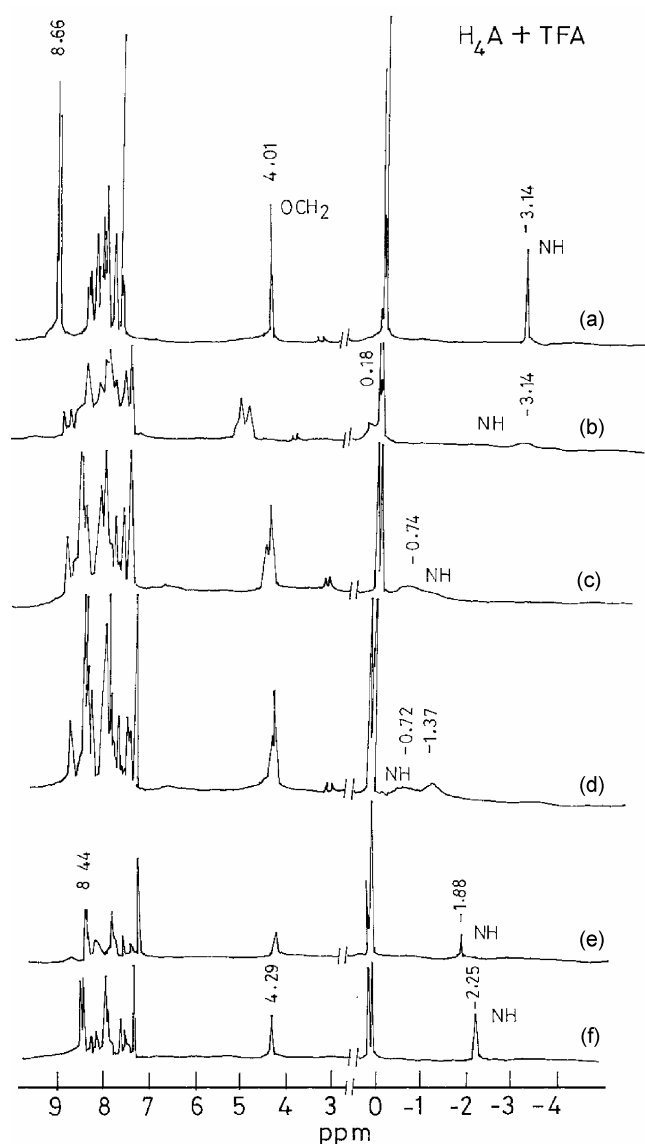


Figure 3. The chemical shifts of proton resonances of H_4A in CDCl_3 at 298 K with increasing addition of TFA. The concentrations of TFA added are: (a) 0.0 M; (b) 0.03 M; (c), 0.07 M; (d) 0.1 M; (e) 0.2 M; (f), neat TFA.

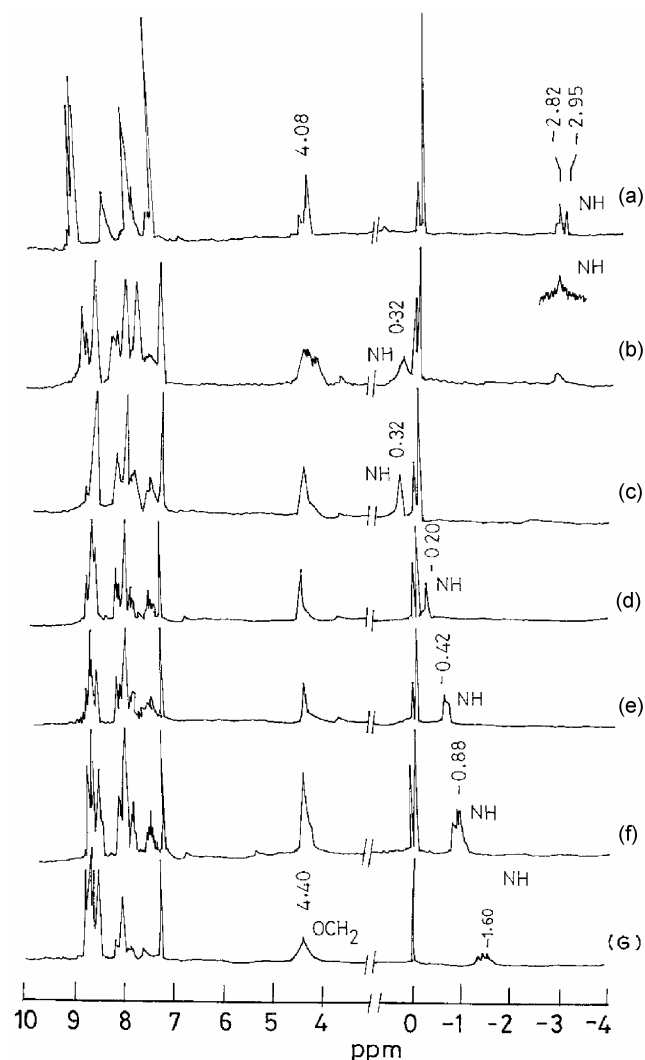


Figure 4. The chemical shifts of proton resonances of H_4B in CDCl_3 at 298 K with increasing addition of TFA. The concentrations of TFA added are: (a), 0.0 M; (b) 0.03 M; (c) 0.05 M; (d) 0.07 M; (e) 0.1 M; (f) 0.2 M; (g) neat TFA.

Table 1. Optical and electrochemical redox data on free-base bisporphyrins and their zinc(II) derivatives in C₂H₄Cl₂ at 298 K.

Compound	λ_{abs} (nm)	$\lambda_{\text{em}}^{\text{a}}$ (nm)	P → P ⁺ (mv)	P ⁺ → P ²⁺ (mv)	P → P ⁻ (mv)	P ⁻ → P ²⁻ (mv)
H ₄ A	415.8 (5.66)					
	514.7 (4.31)	648				c
	549.9 (3.94)	714	+490	+850	-1650	
	589.6 (3.81)	(0.072)		+1070		
	645.6 (3.67)					
H ₄ B	418.1 (5.75)	648				
	514.6 (4.39)	714	+510	+820	-1780	-2060
	549.3 (4.00)	(0.088)		+1020		
	589.0 (3.85)					
	644.0 (3.70)					
Zn ₂ A	415.7 (5.81)	601				
	549.3 (4.42)	650	+310	+650	2030	c
	588.6 (3.71)	(0.002)				
Zn ₂ B	420.0 (5.60)	598				
	549.2 (4.30)	645	+260	+600	c	c
	589.0 (3.69)	(0.018)				

^a $\lambda_{\text{ex}} = 420$ nm. The quantum yields (q) are with reference to H₂TPP and ZnTPP in benzene respectively. ^bThe redox potentials are with reference to Fc⁺/Fc in C₂H₄Cl₂.

^cThe potentials are not observed

the bisporphyrin opens up to fully extended form due to electrostatic repulsion. This movement causes the porphyrin protons to be out of the ring current effect induced by the other unit of the bisporphyrin suggesting expansion of the cavity caused by repulsion due to protonation. This makes all the four N–H protons in each unit chemically non-equivalent in (H₈B⁴⁺) and giving rise to a complex multiplet in TFA. These changes in resonances are connected with distortion of planar porphyrin π -system.¹⁷

The electronic absorption spectra of H₄A and H₄B exhibit characteristic etio type of spectra with the appearance of an intense Soret band (B) in the region 410–420 nm followed by four Q bands (table 1). There is a marginal blue shift of the Soret band (250 cm⁻¹) in H₄A relative to that observed for H₂TPP (monomer) and a general increase in oscillator strength of these bands are suggestive of weak π – π interaction between the porphyrin planes. The fluorescence spectra of H₄A and H₄B and their zinc(II) derivatives exhibit two emissions corresponding to Q_(0,0) and Q_(0,1) bands (figure 5). It is seen that the free-base porphyrins and zinc(II) derivatives exhibit fluorescence with large decrease in intensity and quantum yield relative to that of corresponding monomers.¹⁸ The free-base bisporphyrins H₄A and H₄B exhibit 35% and 20% reduction in the emission intensity respectively, relative to that observed for monomeric H₂TPP. The zinc(II) dimers show a sub-

stantial increase in quenching relative to that observed for the free-base dimers indicating that the inter-ring interaction is enhanced on metallation.

4.2 Redox chemistry

The electrochemical redox studies of H₄A, H₄B and their zinc(II) derivatives reveal the manner in which individual porphyrin rings respond to oxidation/reduction reactions. All the potentials are reversible and involve one electron process unless otherwise stated. The free-base bisporphyrins exhibit two-electron first ring oxidation process leading to the formation of H₂P⁺–H₂P⁺ and they occur at less positive potential relative to that found for H₂TPP. The second ring oxidation occurs in two successive one-electron steps resulting in H₂P²⁺–H₂P⁺ and H₂P²⁺–H₂P²⁺ species indicating that after the first ring oxidation, the porphyrin rings become distinct leading to discrete steps for the second ring oxidation. (table 1) the first and second ring reduction processes of the free-base bisporphyrins, however, occur in single steps involving two electrons with the possible existence of H₂P⁻–H₂P⁻ and H₂P²⁻–H₂P²⁻ respectively. This suggests that the reduction steps do not distinguish of the porphyrin rings. The ring oxidation and reduction for zinc(II) derivatives of the bisporphyrins appear as broad peaks and involve two-electron processes. This is unlike those reported for

bisporphyrins containing variable length of covalent linkages.¹⁹ A possible reason for this lies in the marginally longer distance between the two porphyrin

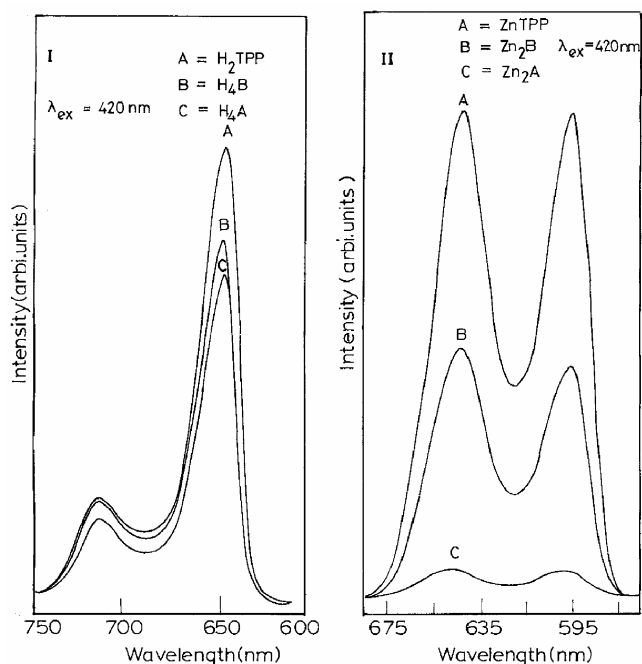


Figure 5. Fluorescence spectra of I, H_4A and H_4B , and II, Zn_2A and Zn_2B bisporphyrins in dichloroethane at 298 K. Excitation at 420 nm.

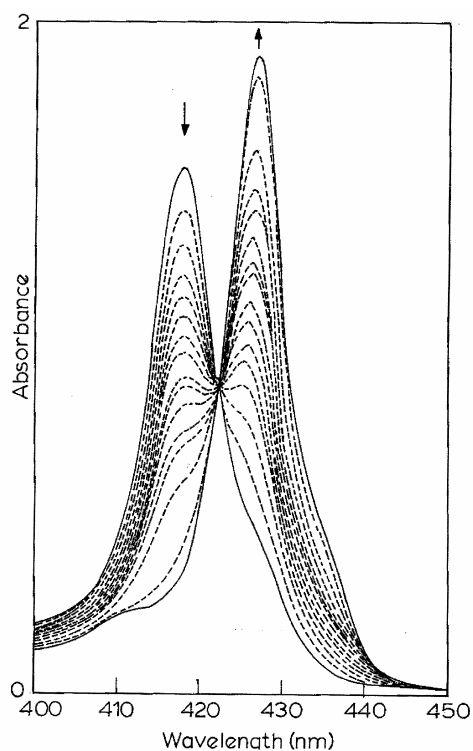


Figure 6. Optical absorption spectra of Zn_2A in dichloroethane on successive addition of PMDA at 298 K.

rings in the metallated derivatives. The second ring reduction occurs at a potential too close to the solvent reduction and hence is not observed. The observation of successive one-electron ring oxidation in the free-base porphyrin, H_4A suggests that the nature of the pre-oxidised species at the electrode surface is quite different from those of zinc(II) derivative.

5. Axial ligation studies

The absorption spectra of Zn_2A on increasing concentration of PMDA are shown in figure 6. The Soret band of the free host is shifted from 415 nm to 424 nm and the visible band at 548 nm is shifted to 563 nm in the complex. The progressive decrease in

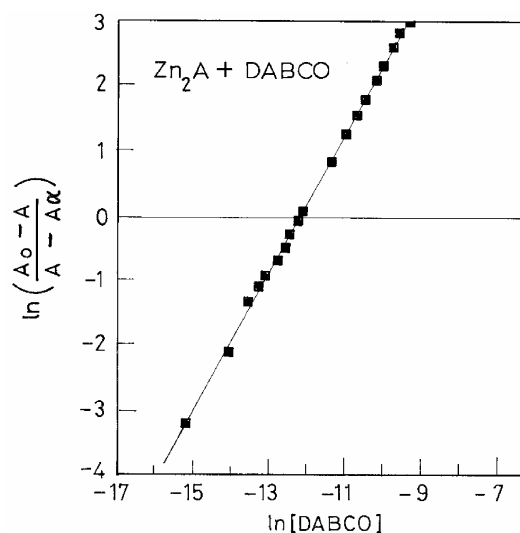


Figure 7. Hill plot of Zn_2A complexation with DABCO.

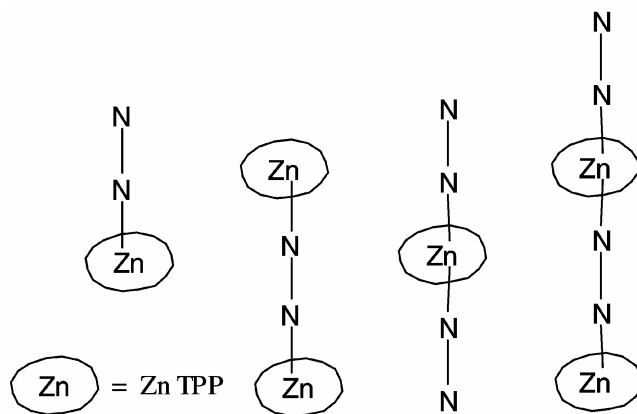


Figure 8. Different possible binding modes of $ZnTPP$ with a bidentate ligand, DABCO.

intensity of absorption bands of the free host, Zn(II) bisporphyrin and increase in intensity of bands corresponding to the complex are monitored as a function of increasing concentration of the bases. The UV-visible spectral changes upon addition of DABCO/PMDA to dichloroethane solution of Zn₂A/Zn₂B showed isobestic points. A representative Hill plot of $\ln(A_o - A)/(A - A_\infty)$ vs $\ln[\text{DABCO}]$, where A_o and A_∞ are the absorbance values at 415 nm of free zinc(II) bisporphyrin and in presence of added base

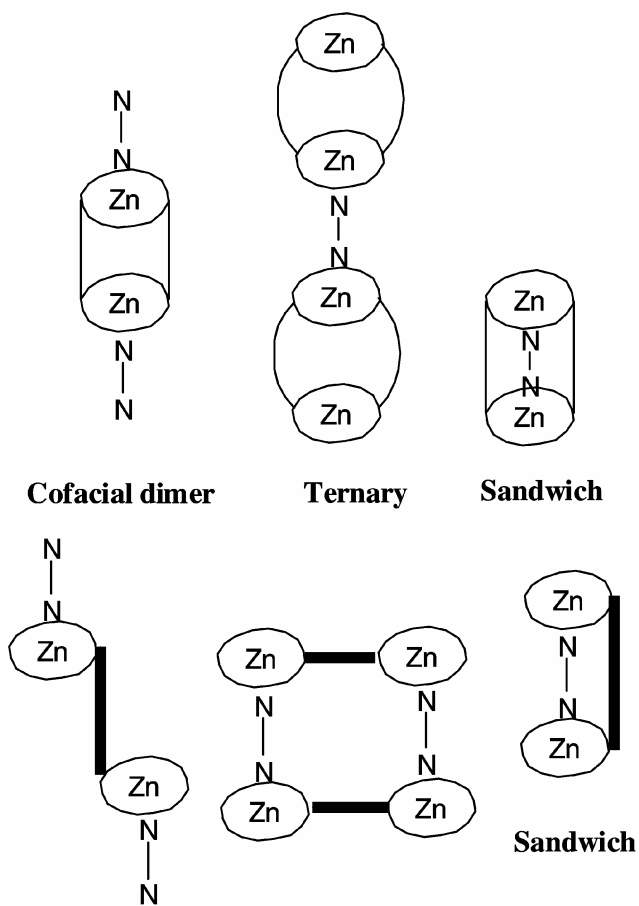


Figure 9. Different modes of binding of Zn(II) bisporphyrins with DABCO.

Table 2. Binding Constants for the axial ligation of bases with Bisporphyrins in C₂H₄Cl₂ at 298 K.

Porphyrin	log K	
	DABCO	PMDA
ZnTPP	5.76	4.62
<i>m-cis</i> -Zn ₂ B	6.70	6.25
<i>m-cis</i> -Zn ₂ B	8.30	8.15

The uncertainty in the values are $\pm 7\%$

respectively, and A is the absorption value of the complex is displayed in figure 7. The linearity of the

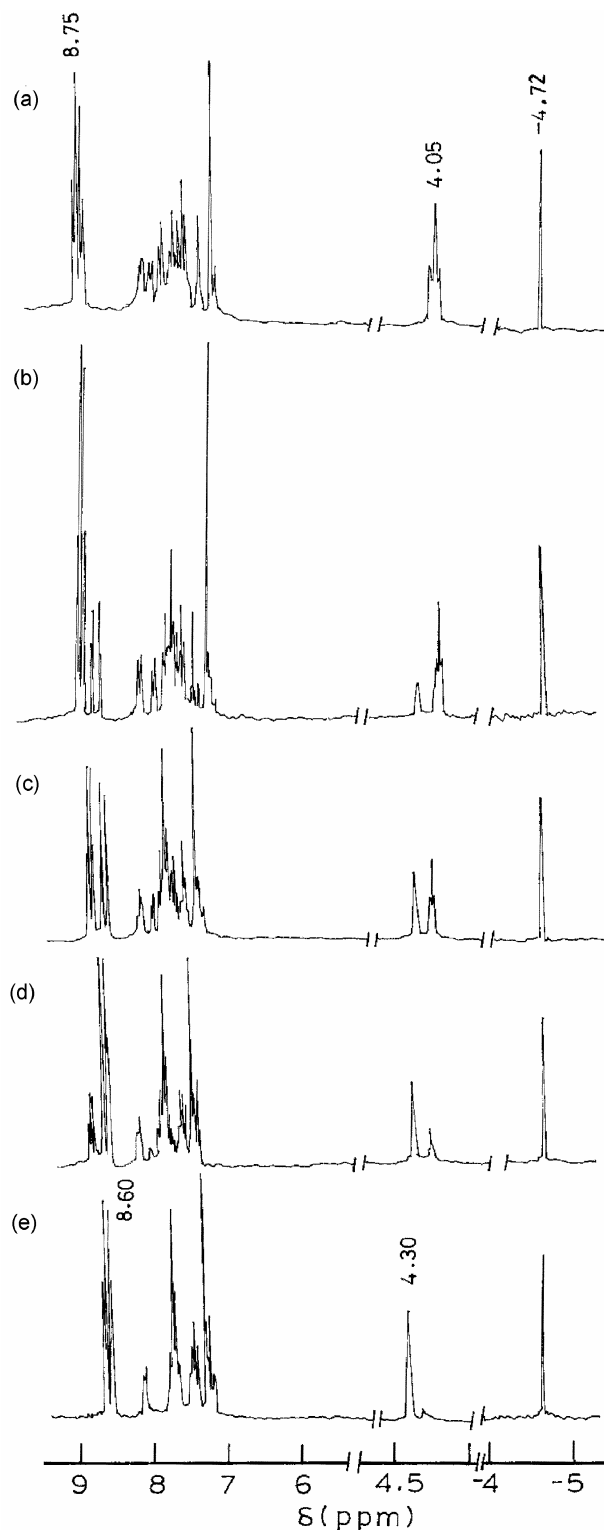


Figure 10. ¹H NMR spectra of CDCl₃ solutions containing different mole ratios of Zn₂A and DABCO. The molar ratio of Zn₂A to DABCO in different spectra are (a) 1 : 0.10; (b) 1 : 0.30; (c) 1 : 0.50; (d) 1 : 0.70; (e) 1 : 1.

plot with a slope of near unity indicates that the predominant species existing in solution is of 1:1 stoichiometry ($Zn_2P:L-L$). The equilibrium constant, K values were evaluated from the intercepts of

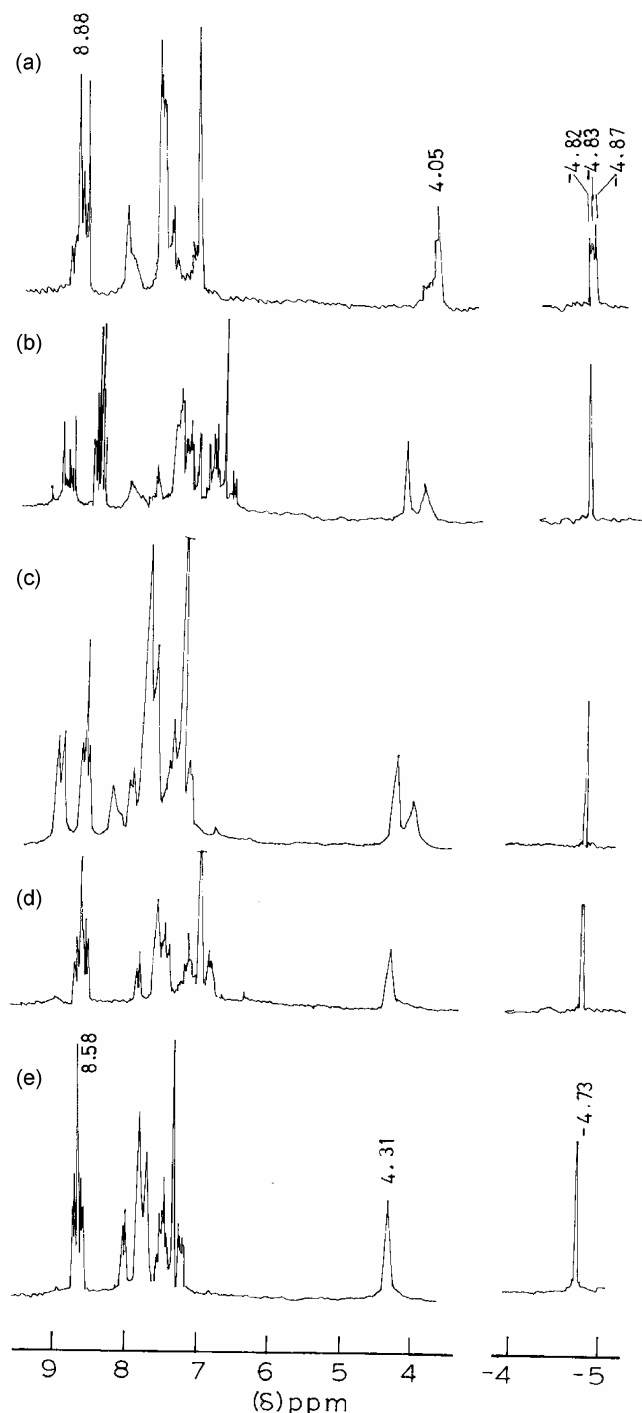


Figure 11. 1H NMR spectra of $CDCl_3$ solutions containing different mole ratios of Zn_2B and DABCO. The molar ratio of Zn_2B to DABCO in different spectra are: (a) 1:0.10; (b) 1:0.30; (c), 1:0.50; (d) 1:0.70; (e) 1:1.

the respective Hill plots. The values of K determined from the increase in absorbance at 424 nm is similar in magnitude to that found by analysing decrease in the absorbance changes at 415 nm.

It is found useful to compare the magnitude of K values obtained for base binding to bisporphyrins with those of monomeric ZnTPP. Experiments were performed under similar conditions to investigate the equilibria of ZnTPP complexation with PMDA/DABCO. The binding curve for the titration of DABCO/PMDA with ZnTPP showed the formation of 1:1 complex. The equilibrium constants for the zinc(II) bisporphyrins with bases are given in table 2 along with the ZnTPP complexation data. The K value for binding of Zn(II) bisporphyrins with DABCO and PMDA are significantly higher than those observed for monomeric ZnTPP and similar in magnitude to those reported earlier.¹³ It is of interest to note that the bisporphyrin, Zn_2B exhibits 1:1 complexation with DABCO and PMDA displaying lower K values relative of Zn_2A -DABCO/PMDA. A possible reason for this lies in the closed conformation associated with the Zn_2A , where the pre-organisation of the host molecule to accommodate a guest molecule is already built-in. In addition, the presence of a rigid bridge between the two binding sites favours complexation to geometrically well defined bidentate ligand. Among the two bidentate ligands, larger K values are observed for binding of DABCO to bisporphyrins relative to the binding of PMDA. This is understandable due to higher chelating factor of DABCO relative to PMDA.²⁰

The complexation of bidentate ligands to zinc(II) derivatives of the bisporphyrins is followed by 1H NMR studies. The proton resonance feature of DABCO binding to monoZinc(II) porphyrin, ZnTPP provide a useful approach towards understanding the nature and mode of binding of the ligand to bismetal porphyrins. The methylene proton resonances of DABCO resonate as a singlet at 2.27 ppm in $CDCl_3$. Addition of this ligand (0.5 mole) to 1.0 mole of ZnTPP shifts the resonances of methylene protons to -4.75 ppm. Increasing addition (1.0 mole) of DABCO to ZnTPP (1.0 mole) results in the shift of methylene protons to -1.03 ppm and any further addition of the ligand does not result in any significant shift of these proton resonances. These observations are interpreted in terms of different modes of binding of bidentate ligand to ZnTPP (figure 8) which can be visualised as follows: a binary complex in which only one donor nitrogen of DABCO is coor-

Table 3. Selected bond lengths (Å) and angles for Zn₂A·DABCO. 8C₂H₄Cl₂·H₂O with esd's in parentheses*.

Zn1–N1	2.085(10)	C3–C4	1.476(21)
Zn1–N2	2.069(7)	C4–C5	1.411(17)
Zn1–N3	2.112(9)	C5–C6	1.530(19)
Zn1–N4	2.085(7)	N1–C1	1.397(15)
Zn1–N5	2.222(7)	N1–C4	1.407(15)
C1–C2	1.449(22)	C2–C3	1.368(17)
NS–C50	1.488(26)	N5–C51	1.445(25)
N5–C52	1.637(33)	O1–C19	1.376(15)
O2–C41	1.327(13)	O2–C45	1.449(15)
C45–C46	1.501(18)	C46–C47	1.495(18)
C47–C48	1.545(18)	C48–C49	1.488(18)
N4–Zn1–N5	99.8(3)	C1–N1–C4	105.0(9)
N3–Zn1–N4	87.5(3)	O2–C41–C42	126(1)
N2–Zn1–N4	160.2(3)	O2–C45–C46	108.5(9)
Zn1–N1–C1	127.4(7)	N1–C1–C2	110(1)
Zn1–N2–C12	125.9(7)	C1–C2–C3	109(1)
Zn1–N5–C52	109(1)	C45–C46–C47	115(1)
C46–C47–C48	114(1)	C47–C48–C49	114(1)

*Ref. 28

minated to Zn(II) while the other nitrogen remain unbound. Alternately, the two donor sites (of DABCO) situated opposite to one another can bind two Zn(II) centers independently resulting in a ternary complex.^{2a} It is possible to conceive hexa coordinated Zn(II) ion in which case a coordinated aggregate and/or a mixture of five and six coordinated structure can result. The optical absorption data clearly indicates the existence of five coordinated zinc(II) and hence we limit our discussion only to five coordinated species. It is found that at low concentration of DABCO, the methylene protons are considerably shielded (by 8.00 ppm) indicating that the ligand protons are restricted in space and come under the influence of strong ring current effect imposed by the donor porphyrins. This situation is well-represented in the ternary structure. Increasing addition of DABCO to ZnTPP (1 : 1 mole) reduces the magnitude of the shift of methylene proton resonances to 3.30 ppm suggesting that the ring current effect experienced by these protons is diminished. This is consistent with that of a binary complex wherein only one porphyrin unit is involved in causing the ring current shift of the resonances. This suggests that the magnitude of the shift of ligand proton resonances provide information on the modes of coordination of DABCO to zinc(II) porphyrins. We shall return to our study on the complexation of DABCO with two Zn(II) derivatives of the bisporphyrins. The conceivable modes of coordination is depicted in figure 9. The spectral changes brought about by

complexation of DABCO with Zn₂A/Zn₂B are displayed in the figures 10 and 11 respectively. Initial addition of 0.3 mole of DABCO to one mole of the zinc(II) bisporphyrins results in the existence of proton resonances that can be ascribed to both the complexed DABCO species and uncomplexed bisporphyrins. This is due to the slow exchange between the free host and complexed species as revealed by large equilibrium constant ($\log K \sim 8.20$) determined by optical absorption method. Increasing addition of DABCO, up to 1.0 mole, results in the slow disappearance of the proton resonances of uncomplexed bisporphyrins with the predominant existence of the complexed species. Addition of DABCO beyond 1.0 mole results in the appearance of proton resonances of free DABCO at 2.27 ppm and bound DABCO at –4.75 ppm, indicating fast exchange between bound and free DABCO in solution.

It is of interest to note that in solutions containing $[DABCO] < Zn_2A/Zn_2B$, the methylene proton resonances of DABCO appear as a singlet at –4.72 ppm in the case of Zn₂A complexation (figure 10) and three singlets at –4.82, –4.83 and –4.87 ppm for Zn₂B complexation (figure 11). The existence of single resonance for the ligand protons in the complexation with Zn₂A indicates the formation of an unique complex while the appearance of multiple resonances of DABCO in Zn₂B complexation is possibly related to the coexistence of different complexes of varying structures. The large magnitude of shielding (~8.00 ppm) experienced by the methylene protons of

DABCO in Zn_2A complex suggests that these protons are situated well within the strong ring current zone of the two porphyrin units consistent with the sandwich structure. We attribute the resonances at -4.87 , -4.83 and -4.82 ppm to ternary, sandwich and binary complexes respectively. It is worthy to mention here that Zn_2B , unlike Zn_2A can exist in different conformations and hence the approach of DABCO towards the Zn(II) ions of bisporphyrin varies considerably resulting in different structures. It is important to observe that the resonance of methylene protons of DABCO remain unshifted (-4.72 ppm) despite increasing the ratio of the ligand to Zn_2A . However, under the same conditions, the three distinct resonances of DABCO bound to Zn_2B are collapsed to a single resonance at -4.73 ppm. This indicates the different modes of binding of the ligand in Zn_2B -DABCO complex existing at low concentration of the ligand are transformed to the sandwich structure at higher concentration. The conformational changes of Zn_2A/Zn_2B during complexation with DABCO are discernible in the shifts of resonances of bridging $-OCH_2-$ protons of the hosts, pyrrole protons and *meso* phenyl groups. The upfield shift (~ 0.30 ppm) of the $-OCH_2-$ protons and

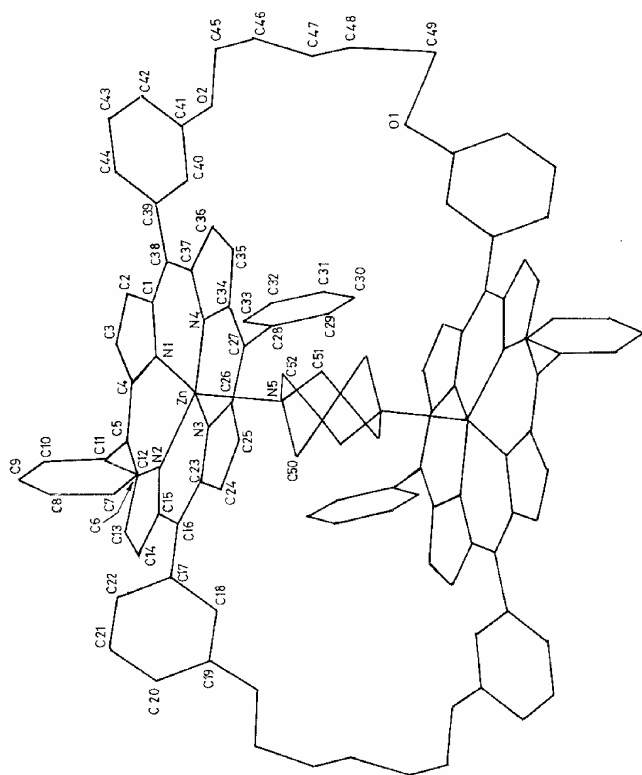


Figure 12. Atomic numbering scheme for the $Zn_2A \cdot DABCO$ complex. The carbon atoms of solvent molecules are not shown.

the complex multiplet resonance of *meso-aryl* protons indicate the skeletal motions of these groups as the ligand being coordinated to the Zn(II) ions. The pyrrole proton resonances of Zn_2A appear as two doublets during complexation with a marginal upfield shift of 0.15 ppm. However, there is a large change in the multiplet structure of the pyrrole proton resonances of Zn_2B resulting in two doublets and two singlets accompanied by an upfield shift of 0.34 ppm. This observation signifies sandwich structure of the complex with two porphyrin planes facing one another and DABCO interposed between the planes. A possible reason for the absence of large segmental motion of the groups in Zn_2A on complexation with DABCO is related to the pre-existent conformation readily available for coordination.

Interesting results have been obtained on PMDA complexation with the bisporphyrins. The free PMDA in $CDCl_3$ exhibit resonances at 1.02 (*s*), 2.54 (*t*) and 1.24 (*m*) ppm corresponding to the protons of $-NH_2$, $-CH_2NH_2$ and $-(CH_2)_3$ -groups, respectively. These resonances are shifted upfield on coordination of PMDA to the two Zn(II) ions of the bisporphyrins. At low concentration (ratio of PMDA/ $Zn_2A = 0.5$), the proton resonances of PMDA appear at -5.24 ppm, -3.04 ppm and at -2.39 ppm corresponding to $-NH_2$, $-CH_2NH_2$ and $-(CH_2)_3$ groups, respectively, while for Zn_2B complexation the corresponding proton resonances occur at -5.08 , -2.96 and -2.29 ppm. The large magnitude of the upfield shift of the proton resonances along with the loss in the multiplet structure (relative to the resonances of free ligand arise from the ring current effect induced by the two porphyrin units of the bisporphyrins. Two effects come into operation on increasing the ratio of (PMDA/(Zn_2A/Zn_2B)) beyond 0.5 . Firstly, the line width of the proton resonances of the ligand increases and the broadening of the resonances is relatively higher for Zn_2B than that observed for Zn_2A . Secondly, the proton resonances of the unbound PMDA start appearing at 2.63 ppm. These observations suggest that there is a fast exchange of proton resonances between the unbound and bound PMDA. The proton resonances of the host entities Zn_2A/Zn_2B ($H\beta/OCH_2$) show only marginal downfield shift on complexation with PMDA.

5.1 Crystal structure of $Zn_2A \cdot DABCO$ complex

The host-guest complex $Zn_2A \cdot DABCO \cdot 8C_2H_4Cl_2 \cdot H_2O$ was crystallized in the monoclinic system with

two molecules in the unit cell. The selected bond lengths and angles of the porphyrin skeleton including the axially co-ordinated ligand molecule are given in table 3. Figure 12 depicts the atom numbering scheme, and an ORTEP diagram is shown in figure 13.²⁸ All the atoms in the Zn(II) porphyrin skeleton are well-defined with no significant differences in bond length and bond angles and are similar to monomeric ZnTPP-base crystal structures.²¹ The

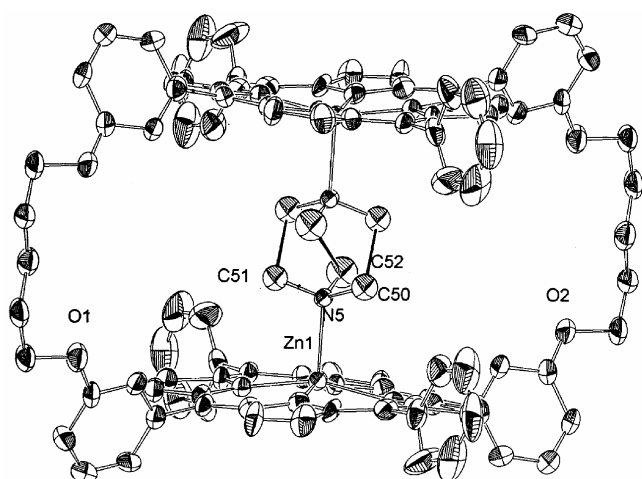


Figure 13. An ORTEP diagram of $Zn_2A \cdot DABCO$ complex with thermal ellipsoids showing 30% probability.

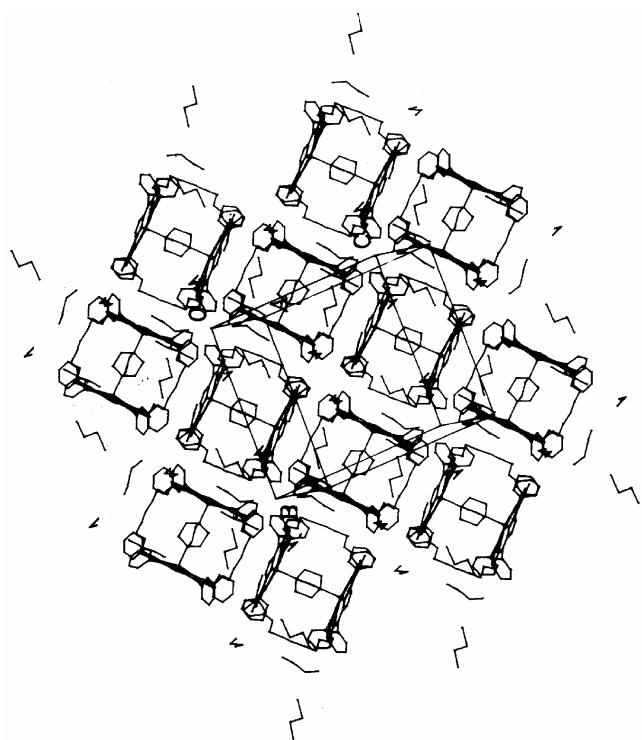


Figure 14. Crystal packing of $Zn_2A \cdot DABCO$ complex.

structure has DABCO encapsulated Zn_2A complex with eight dichloroethane and a water molecule. The molecule indeed accommodates the guest, the central point of which describes a crystallographically imposed center of inversion. DABCO is coordinatively bonded to both Zn atoms of the bisporphyrins. The average Zn–N distances (in the zinc porphyrin) for the complex are 2.08 and 2.22 Å and are similar to those found for a number of axially nitrogen base coordinated Zn(II) porphyrins.²¹ The Zn atom is pulled into the cavity by the nitrogens of DABCO and they are deviating from the mean plane (formed by four pyrrolic nitrogens, N4 plane) by about 0.35 Å. Average distance between the Zn–N (of the DABCO) is found to be 2.22 Å. It can be seen from the ORTEP diagram that DABCO is positionally disordered and the bond distances significantly differs from their normal values. The alkyl linkers are ~20 Å away from each other (figure 13) allowing the molecule to have a large cavity inside the molecule, part of which is filled by DABCO and other solvent molecules. The rest of the cavity assumes a triangular sheet like hole around the DABCO (void volume ~450 Å³). The two alkyl linkers, the midpoint of which defines a virtual two fold axis through the center of DABCO are covalently bonded to the *trans-meta*-hydroxy group of the *meso*-phenyl rings and are essentially planar with the maximum mean plane deviation being 0.08 Å. These bridging groups are parallel to each other and perpendicular to the porphyrin plane. All the carbon atoms of the alkyl group are well ordered and have staggered conformation instead of the more stable *gauche* conformation. This could be related to the moderately strong hydrogen bonding with the porphyrin ring of a nearest neighbour (figure 14). The porphyrin ring is found to be nonplanar. The alternate pyrrole rings are rotated either clockwise or anticlockwise around the Zn–N bonds such that the *meso*-carbons are above and below the mean plane alternatively. The mean deviation of the *meso*-carbon atoms are 0.16, –0.12, 0.18 and –0.13 Å. A parallel arrangement of the mean planes of the porphyrins is observed and is separated by a distance of 7 Å. The observed ruffled conformation of the porphyrin rings in the structure is possibly due to the steric constraints imposed by the *meso*-phenyl substituents or intermolecular interactions with the neighbouring molecules in the lattice. Bisporphyrins without self-complementary shapes does not stabilize the host lattice structure without the incorporation of solvent molecules. So is

the case in this system, where the lattice structure gets stabilized by incorporation of dichloroethane and water molecules in the lattice. In porphyrin sponges, it has been reported that the host lattices have a sheet like cavity through out the lattice which is having π -stacking origin.²² The present structure does not have sheet like channels, and the complementary voids are occupied by the solvent molecules. Majority of the bisporphyrin complexes tend to adopt an offset orientation to minimize π - π repulsion and maximize σ - π attraction.²³ The present structure shows perfect face-to-face stacking of the two Zn(II) porphyrins in an eclipsed configuration with nearly zero offset geometry. No screwed down conformation has been observed between the two porphyrin rings. Another striking feature is that the slippage or lateral displacement of the two Zn atoms are close to zero. This is possibly due to binding of DABCO and outward stretching of the alkyl linkers brings the rings closer to each other thereby increasing π - π interaction.

Acknowledgements

The authors are thankful to the Department of Science and Technology (DST), Government of India for the support. The authors (G V) and (S K M) thank the Jawaharlal Nehru Centre for Advanced Scientific Research, Bangalore for the financial support.

References

- (a) Collman P, Wagenknecht P S and Hutchison J E 1994 *Angew. Chem. Int. Ed. Engl.* **33** 1537; (b) Nam W, Han H J, Oh S-Y, Lee Y J, Choi M-H, Han S-Y, Kim C, Woo S K and Shin W 2000 *J. Am. Chem. Soc.* **122** 8677
- (a) Otsuka S and Yamanaka T (eds) 1988 *Metalloproteins: Chemical properties and biological effects* (Amsterdam: Elsevier); (b) Ravikanth M and Chandrashekar T K 1995 *Structure and Bonding* **82** 105
- (a) Heiler D, McLendon G and Rogalskyj P 1987 *J. Am. Chem. Soc.* **109** 604; (b) Tabushi I and Kugimiya S 1986 *J. Am. Chem. Soc.* **108** 6926; (c) Sessler J L, Johnson M R, Lin T-Y and Creager S E 1988 *J. Am. Chem. Soc.* **110** 3659
- (a) Jeyakumar D and Krishnan V 1992 *Spectrochimica Acta* **A48** 1671; (b) Tian H-J, Zhou Q-F, Shen S-Y and Xu H-J 1993 *J. Photochem. Photobiol. A: Chem.* **163**
- (a) Anderson H L, Hunter C A, Meah M N and Sanders J K M 1990 *J. Am. Chem. Soc.* **112** 5780 and references therein; (b) Danks I P, Lane T G, Sutherland I O and Yep M 1992 *Tetrahedron* **42** 7699; (c) Collman J P, Tyvoll D A, Chang L L and Fish H T 1995 *J. Org. Chem.* **60** 1926
- Chang K, Liu H Y and Abdalmuhdi I 1984 *J. Am. Chem. Soc.* **106** 2725
- Leighton, Cowan J A, Abraham and R J and Sanders J K M 1988 *J. Org. Chem.* **53** 733
- Collman P, Denisevich P, Konai Y, Marrocco M, Koval C and Anson F C 1980 *J. Chem. Soc. Chem. Commun.* 6027
- (a) Collman J P, Anson F C, Bencosme S, Chong A, Collins Y, Denisevich P, Evitt E, Geiger T, Ibers J A, Jameson G, Konai Y, Koval C, Meier K, Oakley P, Pettman R, Schmittou E and Sessler J 1981 *Organic Synthesis: Today and tomorrow* (eds) B M Trost and C R Hutchinson (Oxford: Pergamon Press) 29; (b) Collman J P, Elliot C M, Halbert T R and Tovrog B S 1977 *Proc. Natl. Acad. Sci. USA* **74** 18
- (a) Kagan E, Mauzerall D and Merrifield R B 1977 *J. Am. Chem. Soc.* **99** 5484; (b) Kagan N E 1979 *Porphyrin chemistry advances* (ed.) F R Longo *Ann. Arbor. Sci.* **43**
- Karaman, Blasko A, Almarsson O, Arasasingam R and Bruce T C 1992 *J. Am. Chem. Soc.* **114** 4889
- (a) Landrum, Reed C A, Hatano K and Scheidt W R 1978 *J. Am. Chem. Soc.* **100** 3232; (b) Neumann K H and Vogle F 1988 *J. Chem. Soc. Chem. Commun.* 520; (c) Golubchikov O A, Korovina S G, Kuvshinova E M, Semeikin A S, Shul'ga A M, Perfil'ev V A, Syrbu S A and Berezin B D 1989 *J. Org. Chem. USSR (Engl. Transl.)* 2144
- (a) Hunter A, Meah M N and Sanders J K M 1990 *J. Am. Chem. Soc.* **112** 5773; (b) Anderson H L, Bashall A, Henrick K, McPartlin M and Sanders J K M 1994 *Angew. Chem.* **33** 429; (c) Uemori Y, Nakatsubo A, Imai H, Nakagawa S and Kyuno E 1992 *Inorg. Chem.* **31** 5164; (d) Imai H and Uemori Y 1994 *J. Chem. Soc. Perkin Trans. 2* 1793; (e) Anderson H L and Sanders J K M 1995 *J. Chem. Soc. Perkin Trans 1*, 2223; (f) Anderson H L, Anderson S and Sanders J K M 1995 *ibid* 2231; (g) Anderson S, Anderson H L and Sanders J K M 1995 *ibid* 2247 and 2256; (h) Mackay L G, Anderson H L and Sanders J K M 1995 *ibid* 2269; (i) Wylie R S, Levy E G and Sanders J K M 1997 *Chem. Commun.* 1611
- (a) Chang, Kuo M-S and Wang C-B 1977 *J. Heterocycl. Chem.* **14** 943; (b) Chang C K 1977 *J. Heterocycl. Chem.* **14** 1285; (c) Collman J P, Bencosme C S, Barnes C E and Miller B D 1983 *J. Am. Chem. Soc.* **105** 2704; (d) Collman J P, Denisevich P, Konai Y, Marrocco M, Koval and Anson F C 1980 *J. Am. Chem. Soc.* **102** 6027; (e) Karaman R, Jeon S, Almarsson O and Bruce T C 1992 *J. Am. Chem. Soc.* **114** 4899
- Crossley, Harding M M and Sternhell S 1992 *J. Org. Chem.* **57** 1833
- Sun, Martell A E and Tsutsui M 1986 *J. Heterocycl. Chem.* **23** 561
- (a) Walter I, Ojadi E C A and Linschitz H 1993 *J. Phys. Chem.* **97** 13308; (b) Ojadi E C A, Linschitz H,

- Gouterman M, Walter R I, Lindsey J S, Wagner R W, Droupadi P R and Wang W 1993 *J. Phys. Chem.* **97** 13192
18. Hunter, Leighton P and Sanders J K M 1989 *J. Chem. Soc. Perkin Trans. 1* 547
19. Mest, L'Her M, Hendricks N H, Kim K and Collman J P 1992 *Inorg. Chem.* **31** 835
20. Danks, Sutherland I O and Yap C H 1990 *J. Chem. Soc. Perkin Trans. 1* 421
21. (a) Fleischer C K, Miller L E and Webb 1964 *J. Am. Chem. Soc.* **86** 2342; (b) Glick M D, Cohen G H and Hoard J L 1967 *J. Am. Chem. Soc.* **89** 1996; (c) Scheidt W R, Kastner M E and Hatano K 1978 *Inorg. Chem.* **17** 706; (d) Hatana K, Kawasaki K, Munakata S and Iitaka Y 1987 *Bull. Chem. Soc. Jpn.* **60** 1985
22. Bym, Curtis C J, Goldberg I, Hsiou Y, Khan S I, Sawin P A, Tendick S K and Strouse C E 1991 *J. Am. Chem. Soc.* **113** 6549
23. Hunter and Sanders J K M 1991 *J. Am. Chem. Soc.* **112** 5525
24. Bhyrappa P and Krishnan V 1991 *Inorg. Chem.* **30** 239
25. Hill 1910 *Physiol. London* **40** IV–VII
26. Sheldrick 1986 SHELXS-86 Program for crystal structure determination, University of Gottingen, Republic of Germany
27. Sheldrick 1976 SHELXS-76 Program for crystal structure determination, University of Cambridge, UK
28. Vaijyanthimala G 1996 PhD thesis, see details for figures 12–13, Indian Institute of Science, Bangalore, India